**Cell Reports, Volume *41***

## Supplemental information

# Double knockin mice show NF-κB trajectories in immune signaling and aging

**Shah Md Toufiqur Rahman, Mohammad Aqdas, Erik W. Martin, Francesco Tomassoni Ardori, Preeyaporn Songkiatisak, Kyu-Seon Oh, Stefan Uderhardt, Sangwon Yun, Quia C. Claybourne, Ross A. McDevitt, Valentina Greco, Ronald N. Germain, Lino Tessarollo, and Myong-Hee Sung**

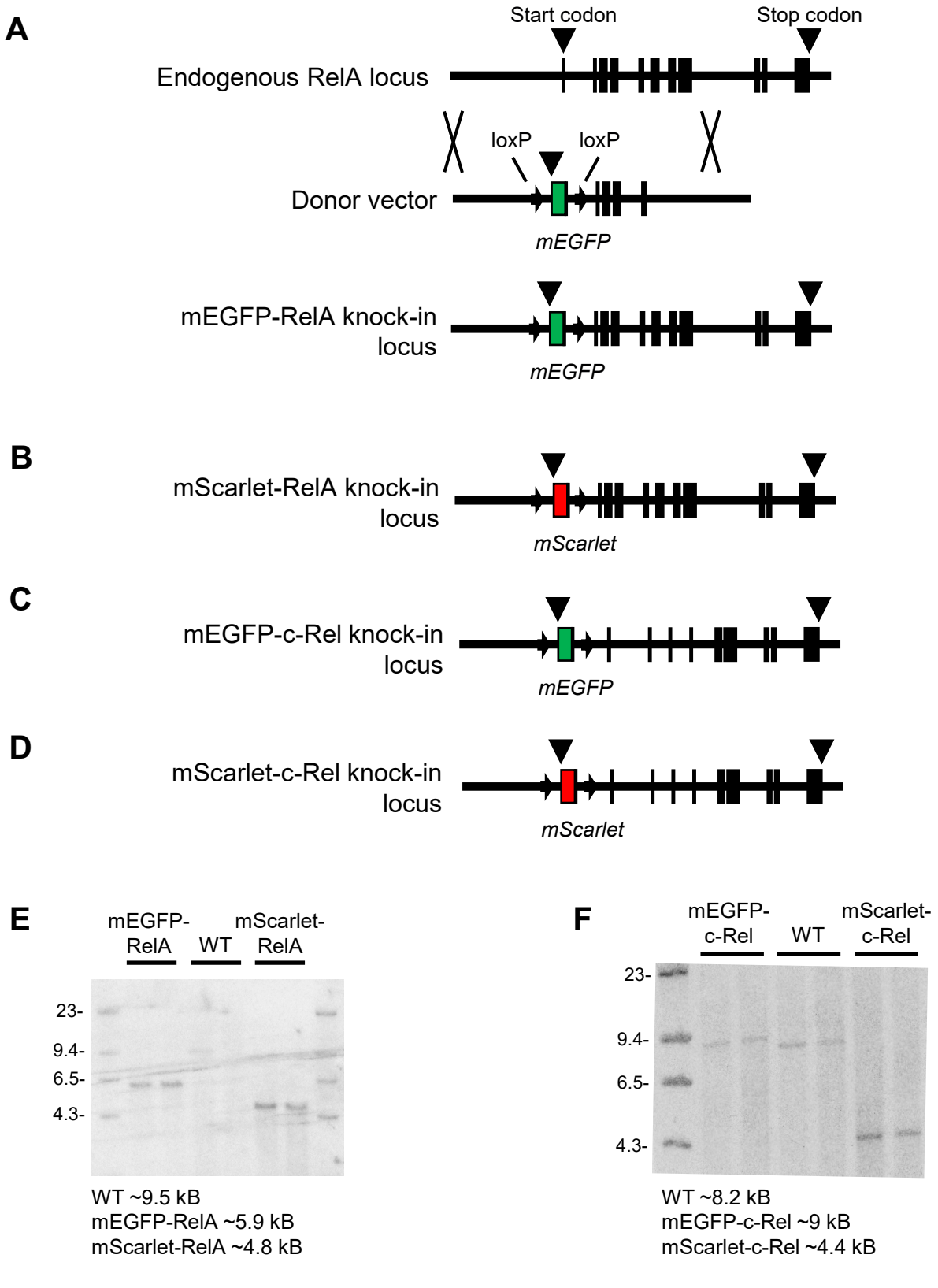


**Supplemental Figure S1. Generation of four endogenous NF-κB knock-in reporter mouse lines (related to Figure 1).**
(A) Schematic of the CRISPR/Cas9-mediated insertion of donor sequence at the start of the *Rela* locus in the mouse genome. The targeted knock-in locus produces the fluorescent fusion protein mEGFP-RelA. (B) The mScarlet-RelA locus, generated with the same strategy as for mEGFP-RelA. (C) The mEGFP-c-Rel locus, generated with a similar strategy targeting the gene start, as for mEGFP-RelA. (D) The mScarlet-c-Rel locus, generated with the same strategy as for mEGFP-c-Rel. (E) Southern blot analysis of RelA knock-in fragments after HincII digestion. 3' probe. (F) Southern blot analysis of c-Rel knock-in fragments after EcoRI digestion. 3' probe.

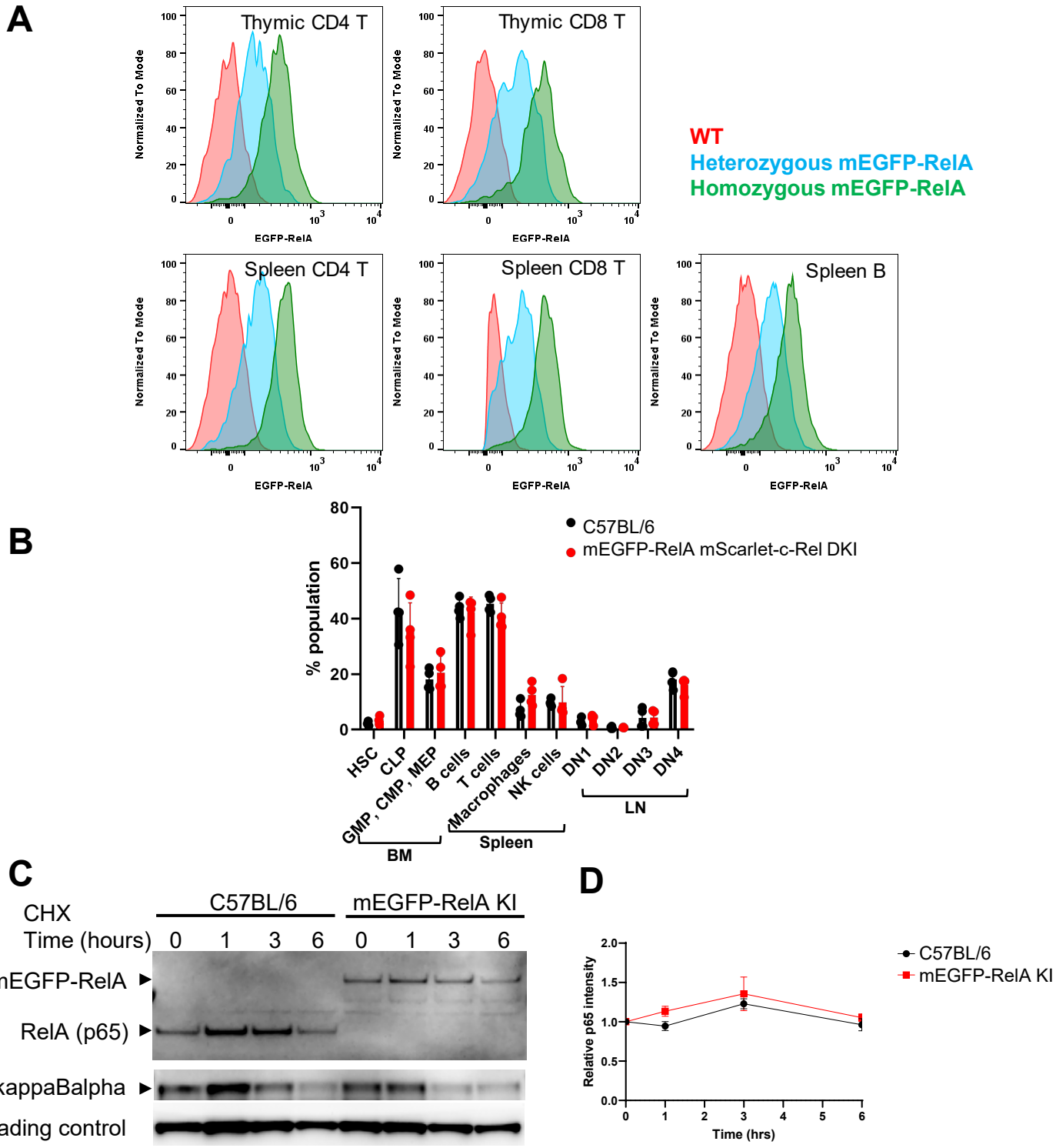


**Supplemental Figure S2. mEGFP-RelA expression, immune cell compositions in knock-in reporter mice, and unaltered stability of the mEGFP-RelA fusion protein (related to Figure 1).**

(A) Flow cytometry of mEGFP-RelA expression in C57BL/6 wildtype, heterozygous knock-in, and homozygous knock-in of mEGFP-RelA. Thymic T cells, spleen T and B cells were analyzed. (B) Cellular compositions (% cells in each population among cells from the indicated tissue) from wildtype and green-red DKI mice are similar. BM: bone marrow, LN: lymph node. Representative of four independent experiments, each with 4 WT and 4 DKI animals. (C) Cyclohexamide (5µg/ml) was used to block new protein synthesis in BMDMs, and abundance of mEGFP-RelA was subsequently monitored by Western blotting for the fusion protein in mEGFP-RelA knock-in mice and for the natural (unlabeled) protein in C57BL/6 mice. IκBα degradation confirms the effectiveness of cycloheximide at the indicated concentration. Loading control was rho-GDI. A representative result is shown from 3-4 independent experiments using different cycloheximide concentrations and time points. Error bars: s.d. of technical replicates. (D) Quantification of data in C using ImageJ. The relative intensity of RelA was normalized to the rho-GDI loading control.

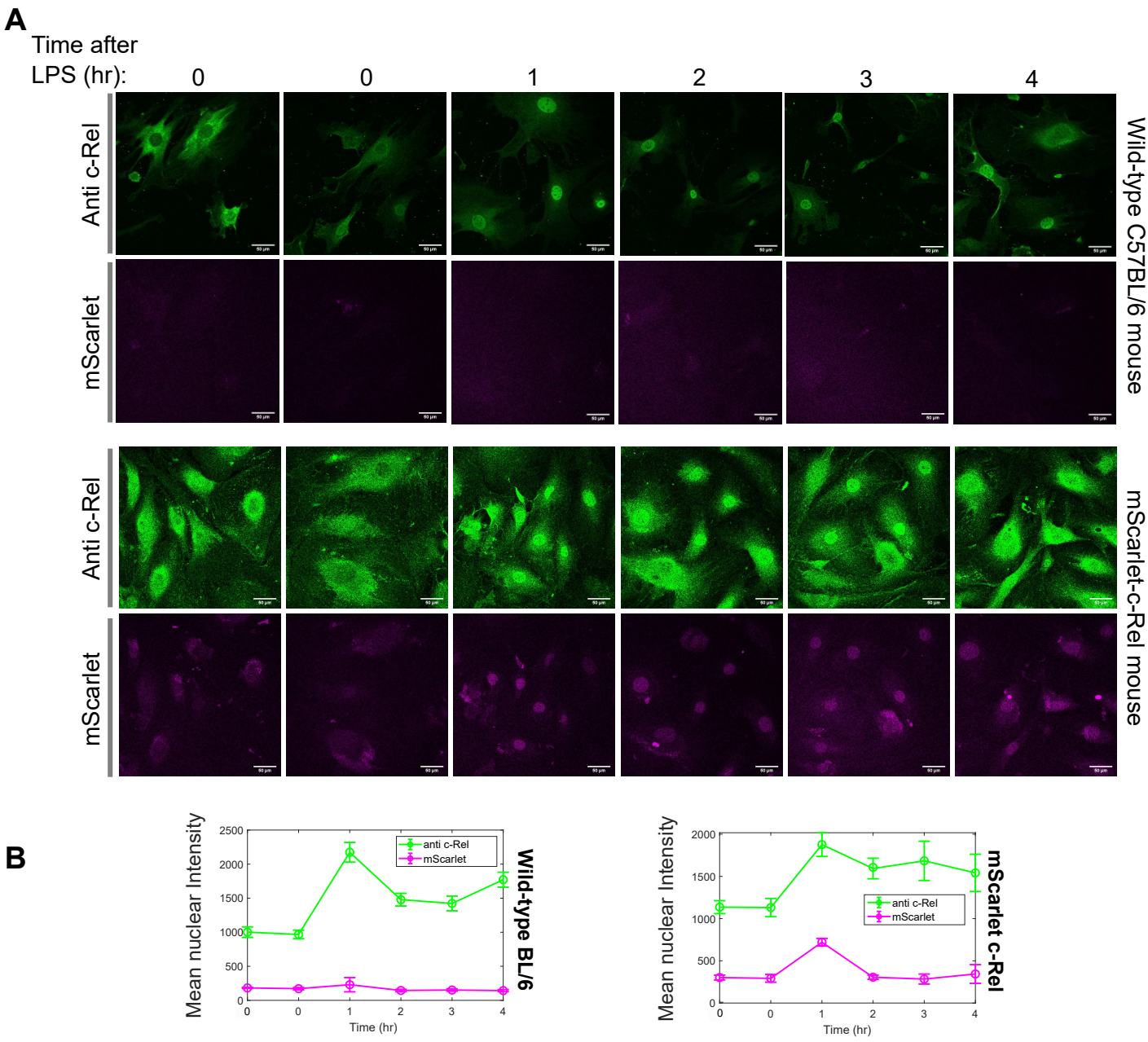


**Supplemental Figure S3. mScarlet-c-Rel signaling is comparable to endogenous c-Rel in wildtype (related to Figure 1).**

(A) Representative images of c-Rel immunofluorescence time-series after LPS (10 ng/ml) stimulation in PEFs isolated from wild-type C57BL/6 mouse (upper panel), or mScarlet-c-Rel knock-in mouse (lower panel). Scale bar = 50 µm. (B) Quantification of c-Rel immunostaining time-series after LPS (10 ng/ml) stimulation in PEFs isolated from wild-type C57BL/6 mouse or mScarlet-c-Rel knock-in mouse. The data represent the mean ± 95% confidence intervals. N (number of quantified cells) = 73, 91, 77, 79, 85, 86 for wild-type C57BL/6; N = 113, 61, 78, 73, 61, 64 for mScarlet-c-Rel.

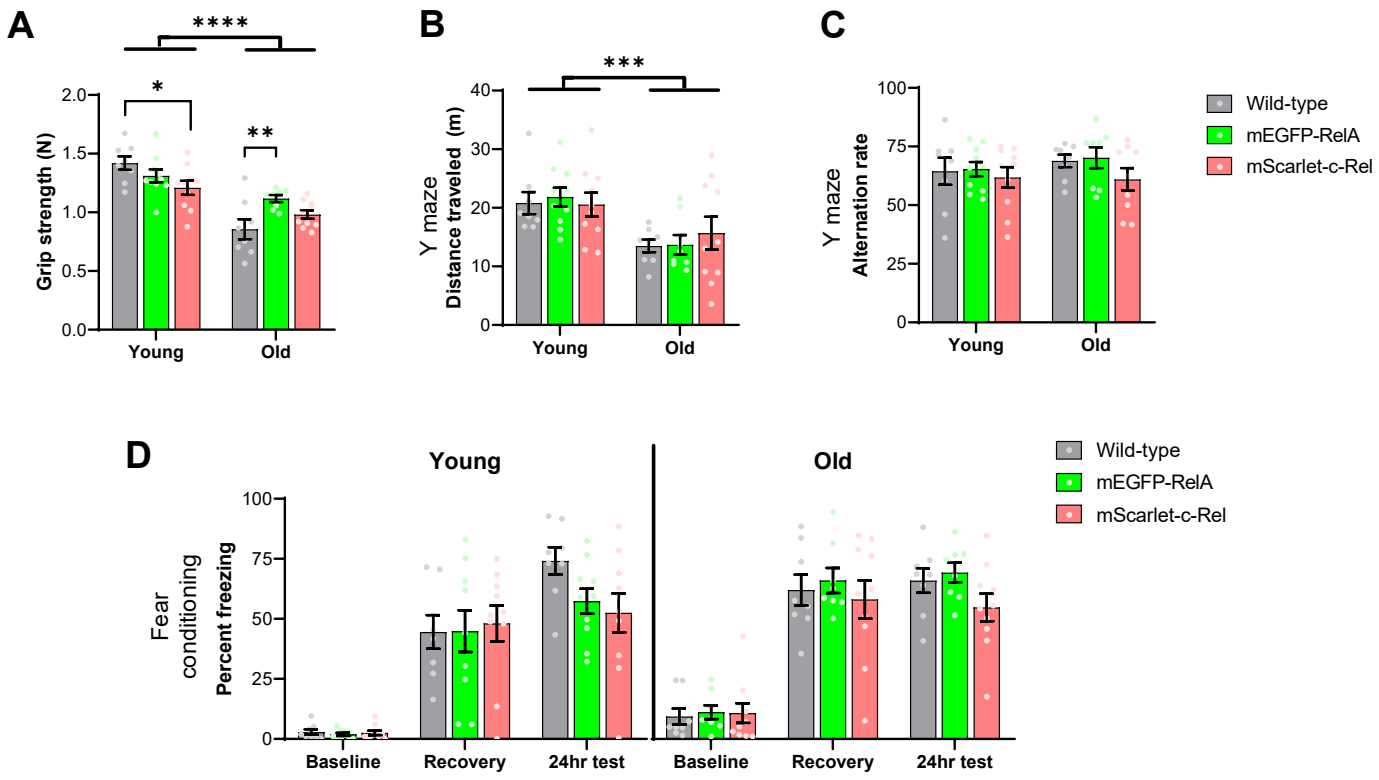


**Supplemental Figure S4. Behavioral testing of mEGFP-RelA and mScarlet-c-Rel mice show phenotypes comparable to wildtype C57BL/6 (related to Figure 1).**

Mice were tested at 3-6 ("young") or 20-30 ("old") months of age. Group sizes were *n*=8-10 mice for each age/strain combination, with approximately equal male/female composition. For statistical analysis, strain, sex and age (in days) were included as interacting model terms; linear modeling was used for data in panels A-C and linear mixed effects modeling for panel D. Post-hoc comparisons were performed using Tukey's HSD with ages grouped categorically into young and old. (A) Forelimb grip strength declined with age (main effect of Age $p$=2.8e-8, ****). The effect of aging varied by strain (Strain × Age interaction $p$=0.0004) and sex (Sex × Age interaction $p$=0.029). Post-hoc comparisons revealed differences between young wild-type versus young mScarlet-c-Rel ($p$=0.037, *) and old wild-type versus old mEGFP-RelA ($p$=0.0072, **). (B) Distance traveled during a 10 minute Y-maze test declined with age (main effect of Age $p$=0.00005, ***). Females were more active than males (main effect of Sex $p$=0.0014). There were no differences between strains. (C) Alternation of arms entries in the Y-maze, a measure of working memory, did not differ by strain, age, or sex. (D) A robust and long-lasting conditioned freezing response was entrained in all groups of mice following delivery of two electric foot shocks in a conditioning chamber (main effect of Phase $p$<0.0001). Freezing was generally higher in aged mice (main effect of Age $p$=0.011). Although there were marginally significant interactions between strain and other factors (Phase × Strain $p$=0.042; Phase × Strain × Age $p$=0.032; Phase × Strain × Age × Sex $p$=0.047), the only significant post-hoc pairwise comparison was a reduction in freezing for female mScarlet-c-Rel versus female wild-type (collapsed across ages) within the 24hr recall test ($p$=0.01).

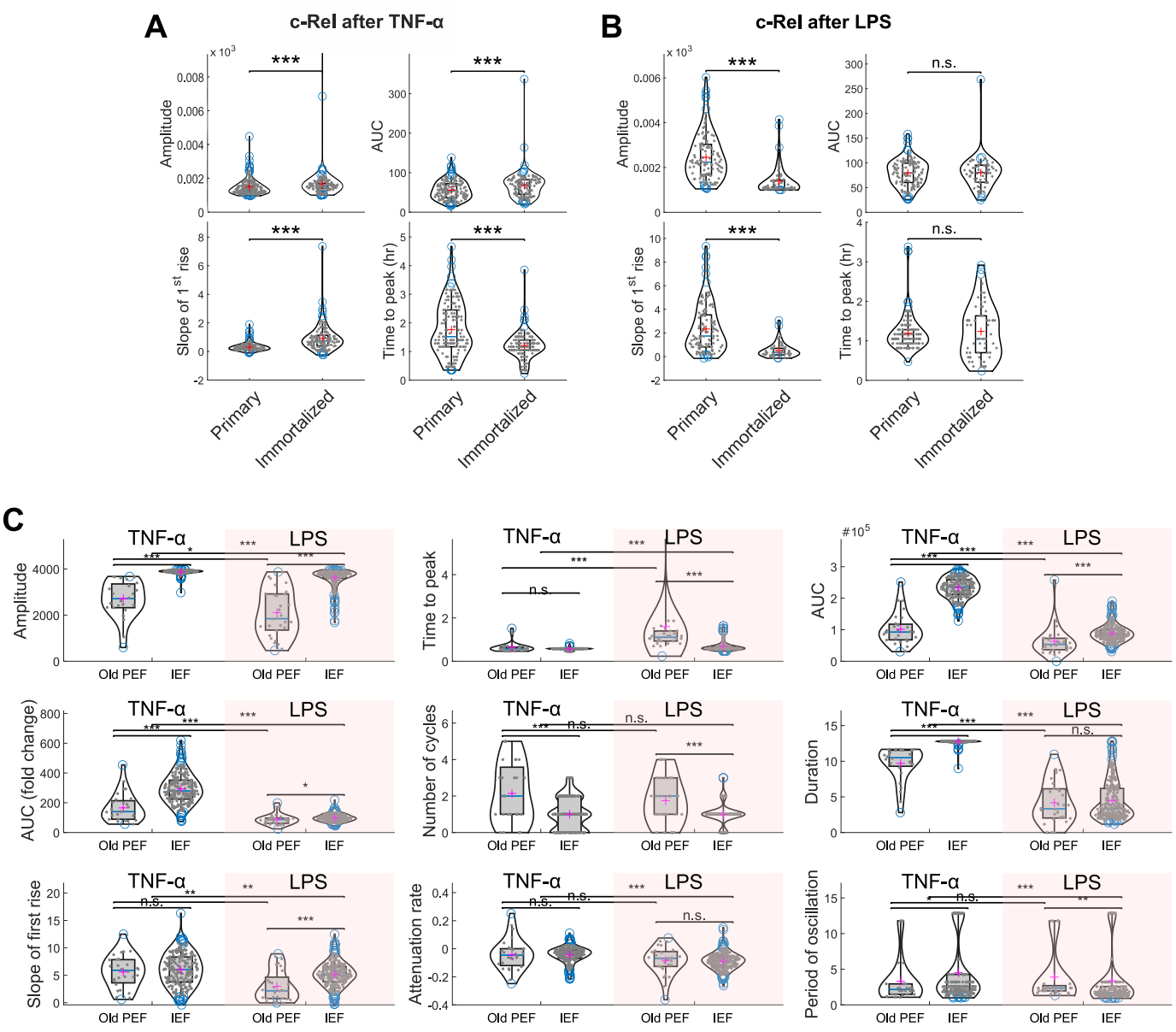


**Supplemental Figure S5. PEFs from aged animals also have distinct signaling dynamics in comparison to IEFs (related to Figure 2).**

(A-B) Quantification of the data in Figure 2, comparing IEFs and PEFs from green-red double knock-in reporter mice. The signaling features of c-Rel in TNF-α-stimulated cells (A) and in LPS-stimulated cells (B). (C) IEFs (n = 245 for LPS and n = 207 for TNF-α) and PEFs (n = 32 for LPS and n = 28 for TNF-α) isolated from an aged green-red double knock-in reporter mouse (92 weeks of age) were imaged as in Figure 2. Cells were stimulated with either LPS or TNF-α. The signaling features of RelA in TNF-α-stimulated cells and in LPS-stimulated cells (shaded in pink).

* $p < 0.05$, ** $p < 0.001$, and *** $p < 0.0001$ from Mann-Whitney U test.

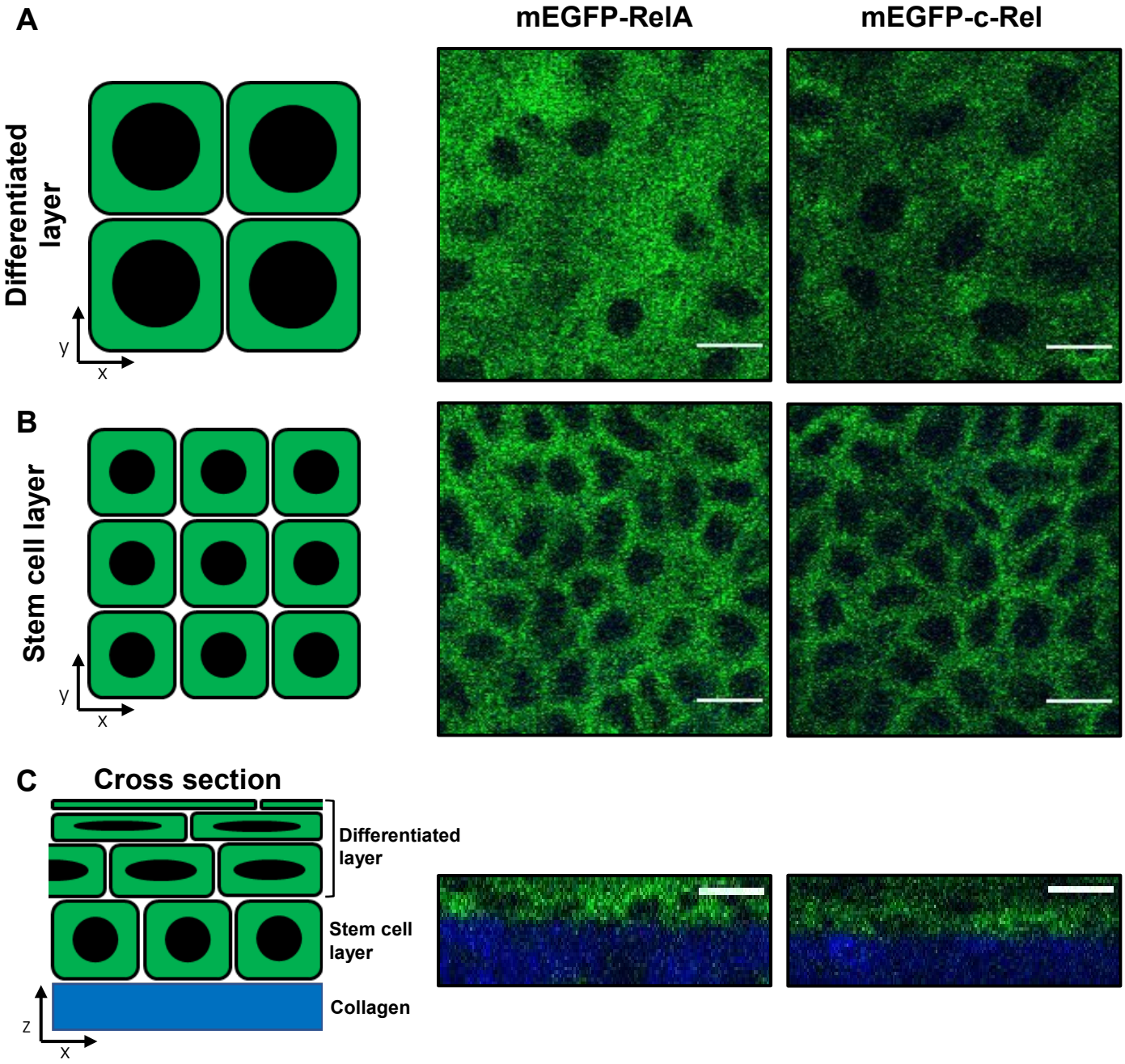


**Supplemental Figure S6. Visualization of RelA and c-Rel in live murine epidermis using two-photon microscopy on mEGFP-RelA and mEGFP-c-Rel knock-in reporter mice (related to Table 1).**
Representative images of the differentiated cell layer (A), stem cell layer (B), and orthogonal cross section (C) from the epidermis of adult, anesthetized mice homozygous for either the mEGFP-RelA or mEGFP-c-Rel knock-in reporter from two-photon microscopy. The differentiated layer includes spinous, granular, and cornified cells deriving from basal cells of the stem cell layer. Scale bar = 10 μm.

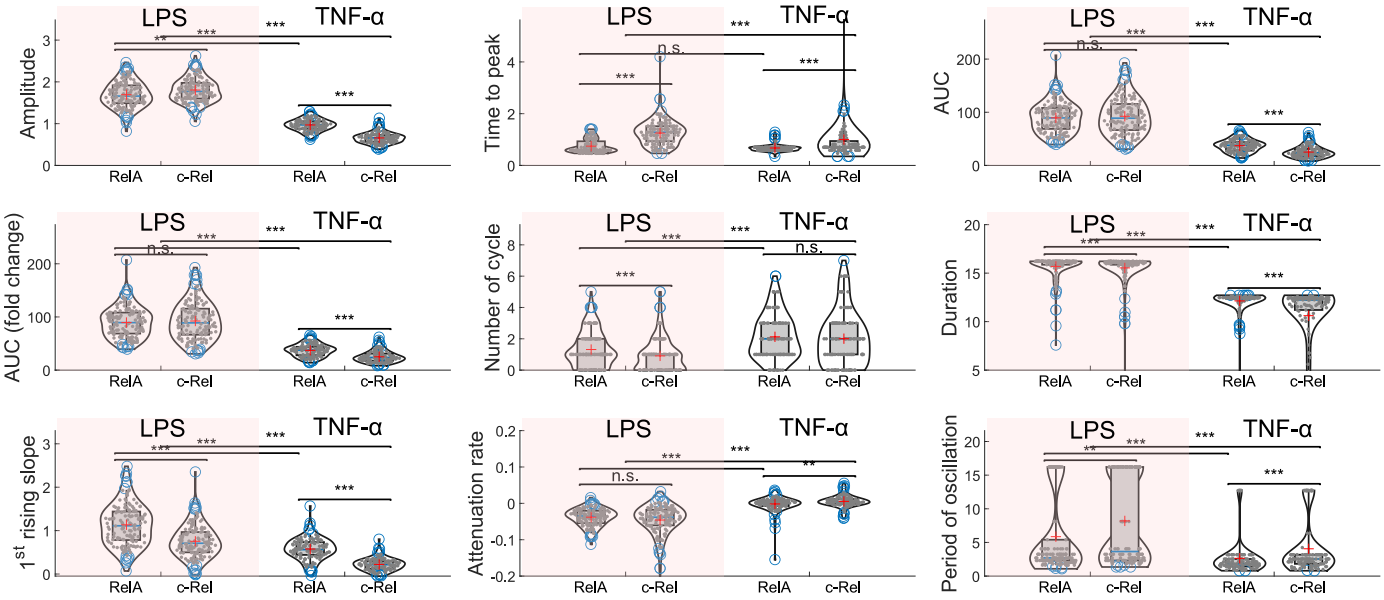


**Supplemental Figure S7. Subunit-specific features of NF-κB signaling in BMDMs following LPS and TNF-α stimulation (related to Figure 3).**

Violin plots show the dynamic features of RelA and c-Rel signaling in LPS- (shaded in pink) and TNF-α -stimulated BMDMs from green-red DKI mice, quantified from data shown in Figure 3.

n.s., not significant, ** $p < 0.001$, *** $p < 0.0001$ from Mann-Whitney U test.

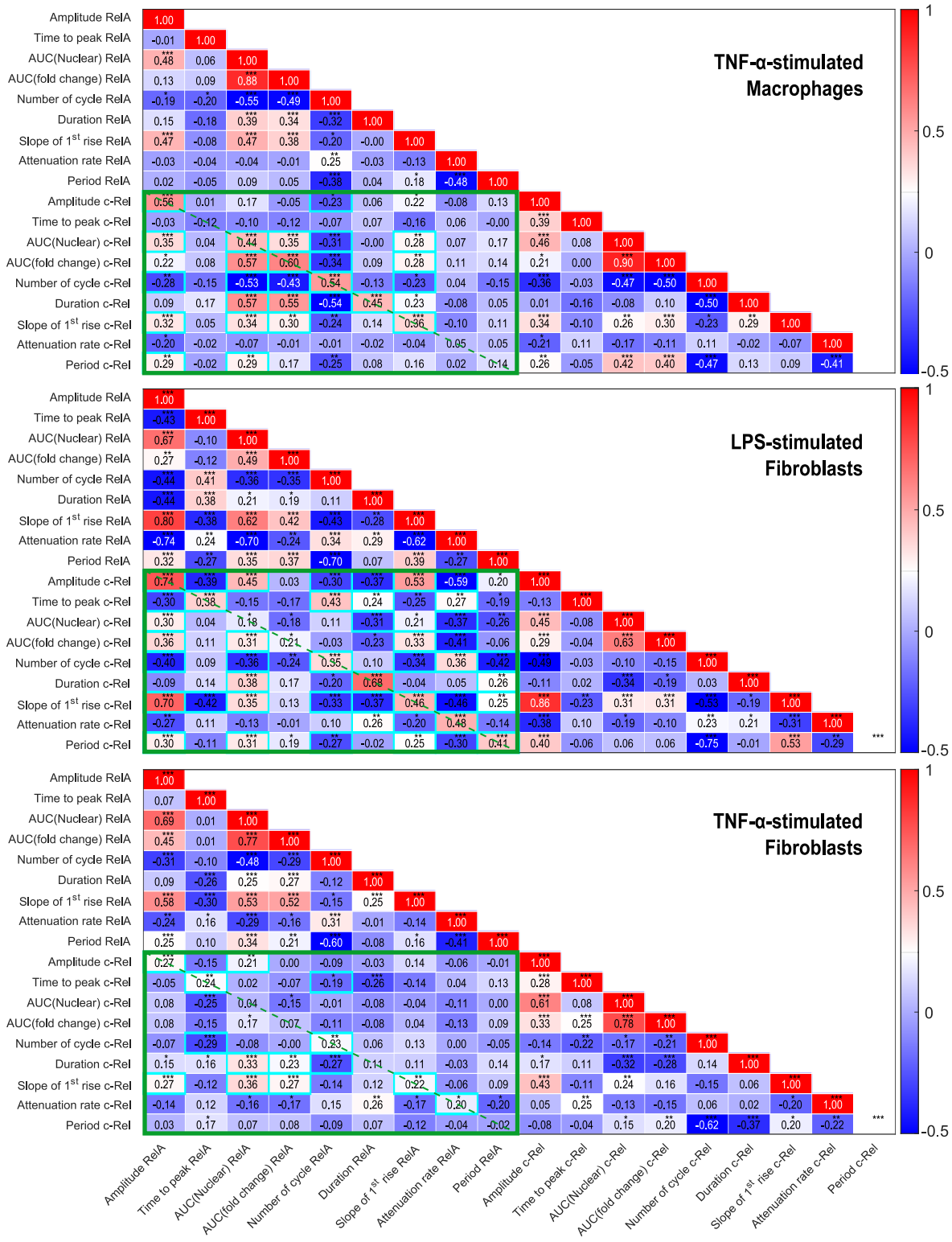


**Supplemental Figure S8. Correlation matrices of RelA and c-Rel signaling features (related to Figure 3).** Correlation matrix heatmaps of RelA and c-Rel signaling features summarize all pairwise correlation analyses from TNF-α-stimulated BMDMs (top), LPS-stimulated fibroblasts (middle), and TNF-α-stimulated fibroblasts (bottom). The individual correlation coefficient is shown inside each cell and * denotes statistical significance (* $p < 0.05$, ** $p < 0.001$, and *** $p < 0.0001$). The green boxes mark RelA & c-Rel cross-correlations. The dashed diagonal lines indicate cross-correlations between the same signaling features of RelA and c-Rel. Cyan boxes indicate permutation test p value was less than 0.01 from 100 random shuffles of RelA:c-Rel same-cell pairing.

**A**

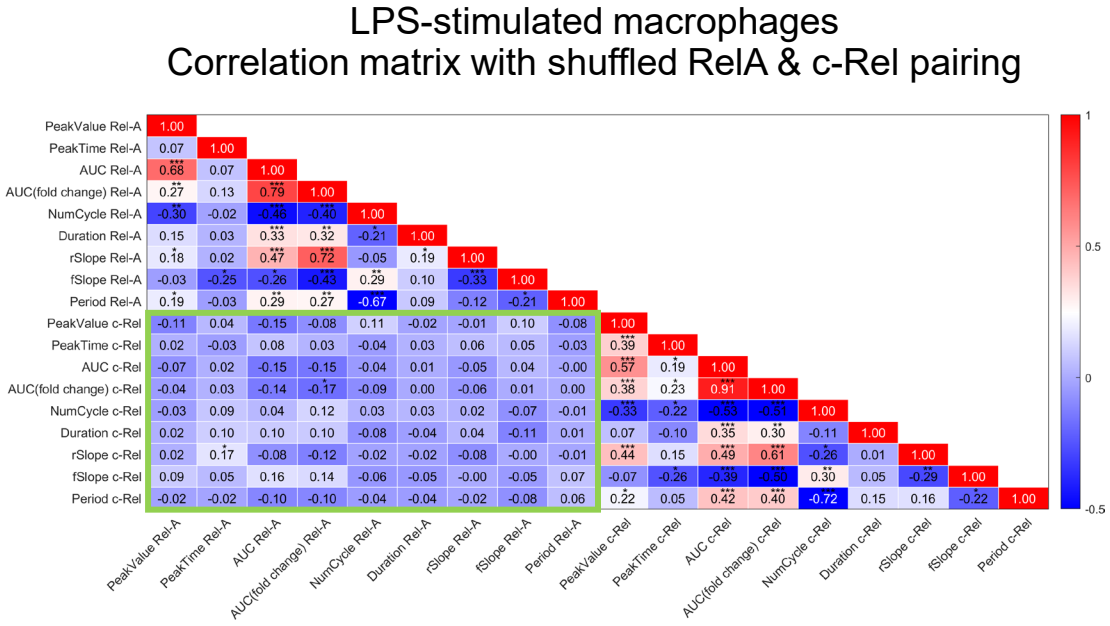


**B**

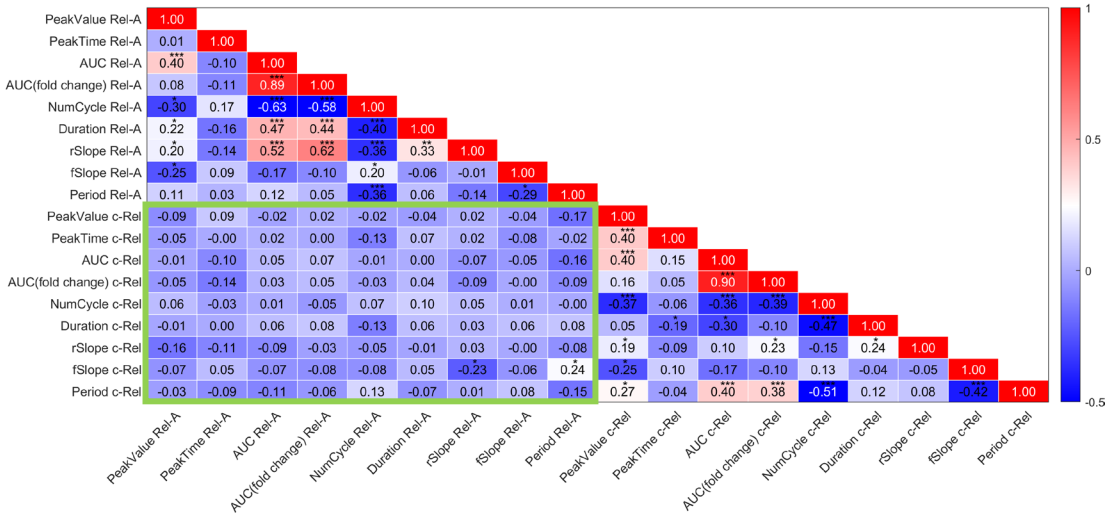


**Supplemental Figure S9. Same-cell measurement of RelA and c-Rel signaling features is required for the observed significant cross-correlations within the correlation matrices (related to Figure 3).** The same-cell pairing of RelA time series and c-Rel time series was randomly shuffled, and the correlation matrix was recalculated for live cell imaging data from LPS-stimulated BMDMs (A) or TNF-α-stimulated BMDMs (B). The green boxes in (A) and (B) mark the lack of RelA & c-Rel cross-correlations in comparison to Figure 3C and the top panel of Figure S8, respectively.

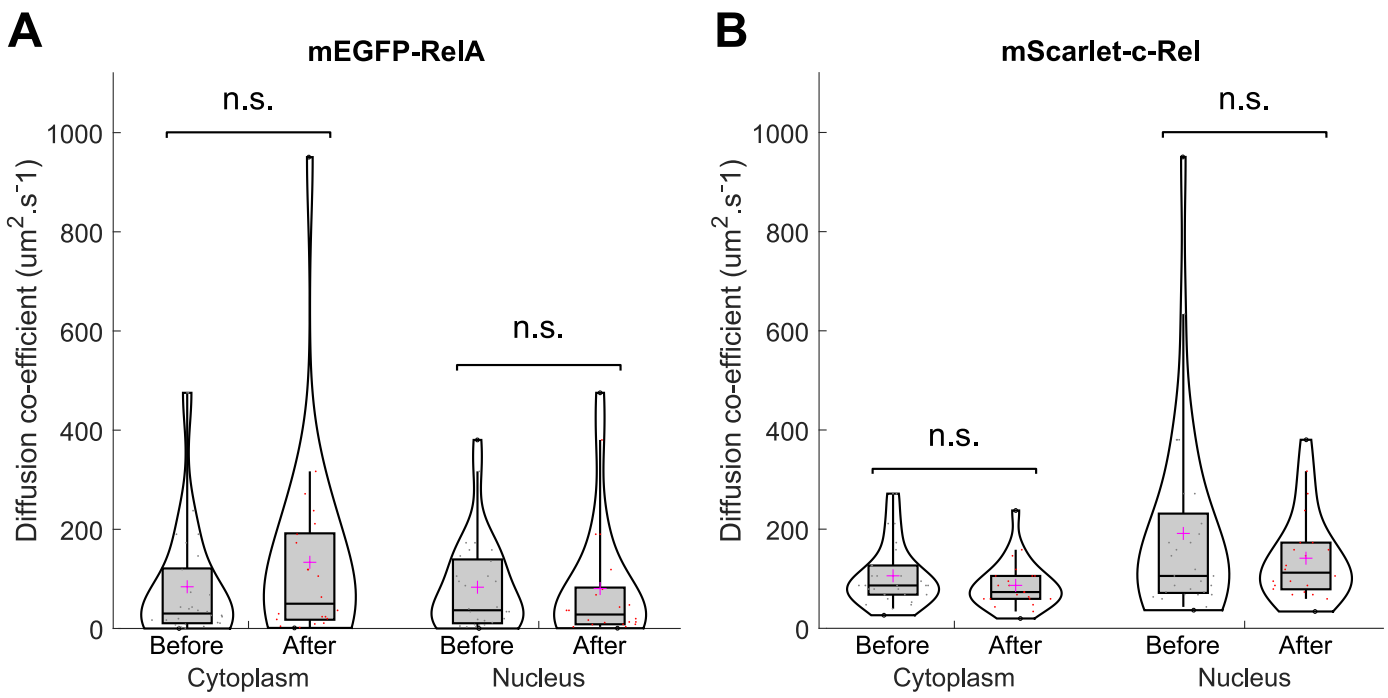


**Supplemental Figure S10. Fluorescence cross-correlation spectrocopy analysis of RelA and c-Rel (related to Figure 4).**

Primary ear fiboblasts from the green-red double knock-in mice were subject to FCCS. The analysis was performed before and after stimulation with TNF-α. (A) Diffusion coefficients estimated from fitting mEGFP-RelA FCS data with a simple diffusion model. (B) Diffusion coefficients estimated from fitting mScarlet-c-Rel FCS data with a simple diffusion model.

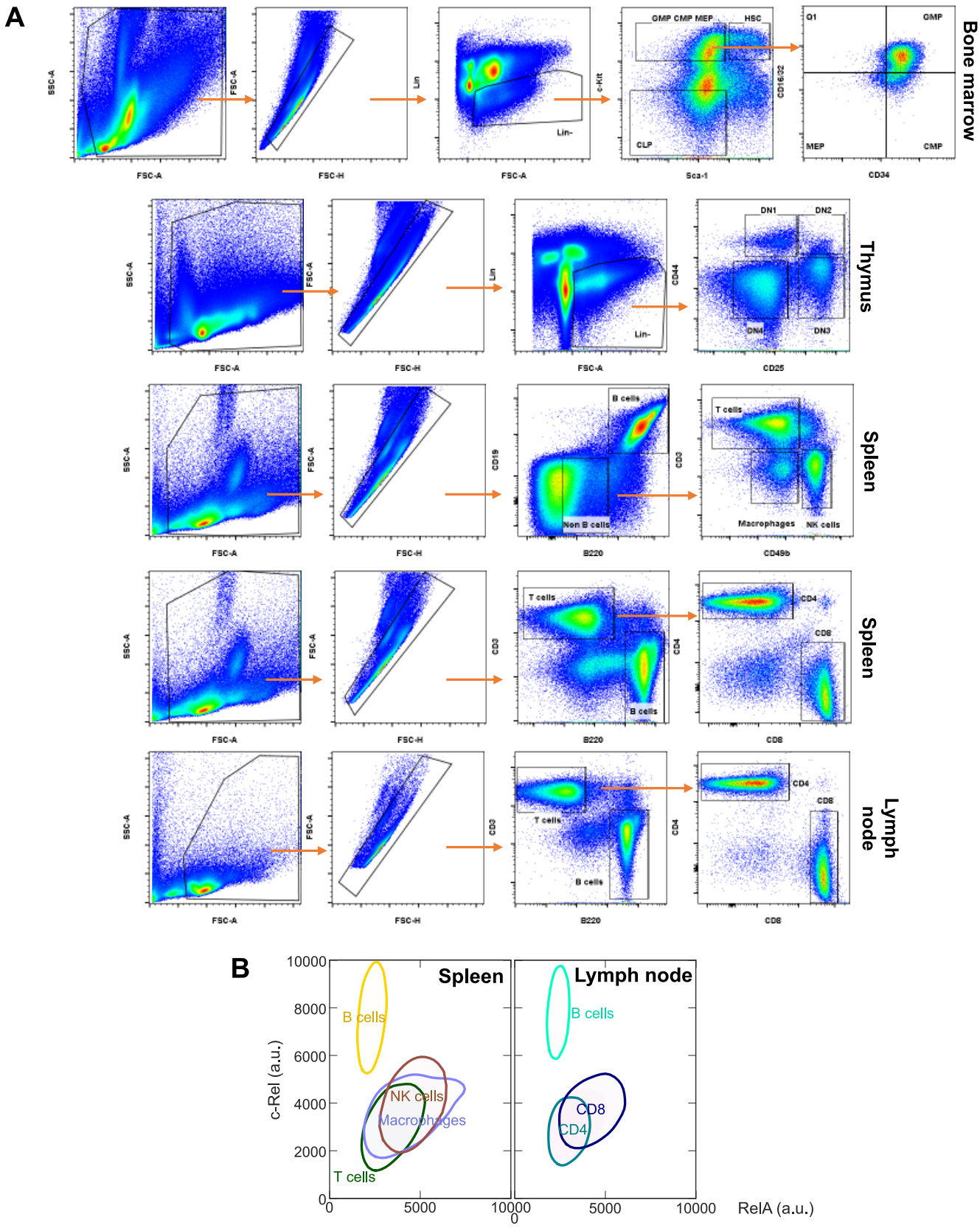


**Supplemental Figure S11. Flow cytometry gating strategies and source organs for immune cell subsets (related to Figure 5).**

(A) Gating strategies are shown for bone marrow, thymus, spleen, and lymph nodes harvested from the green-red double knock-in reporter mice.

(B) RelA and c-Rel abundances are similar for a given cell type (B cells or T cells), regardless of the source organs. Mean RelA and c-Rel fluorescent intensities are coomparable from the same-day flow cytometry experiment, without batch effects. A representative result of three biological replicate experiments.

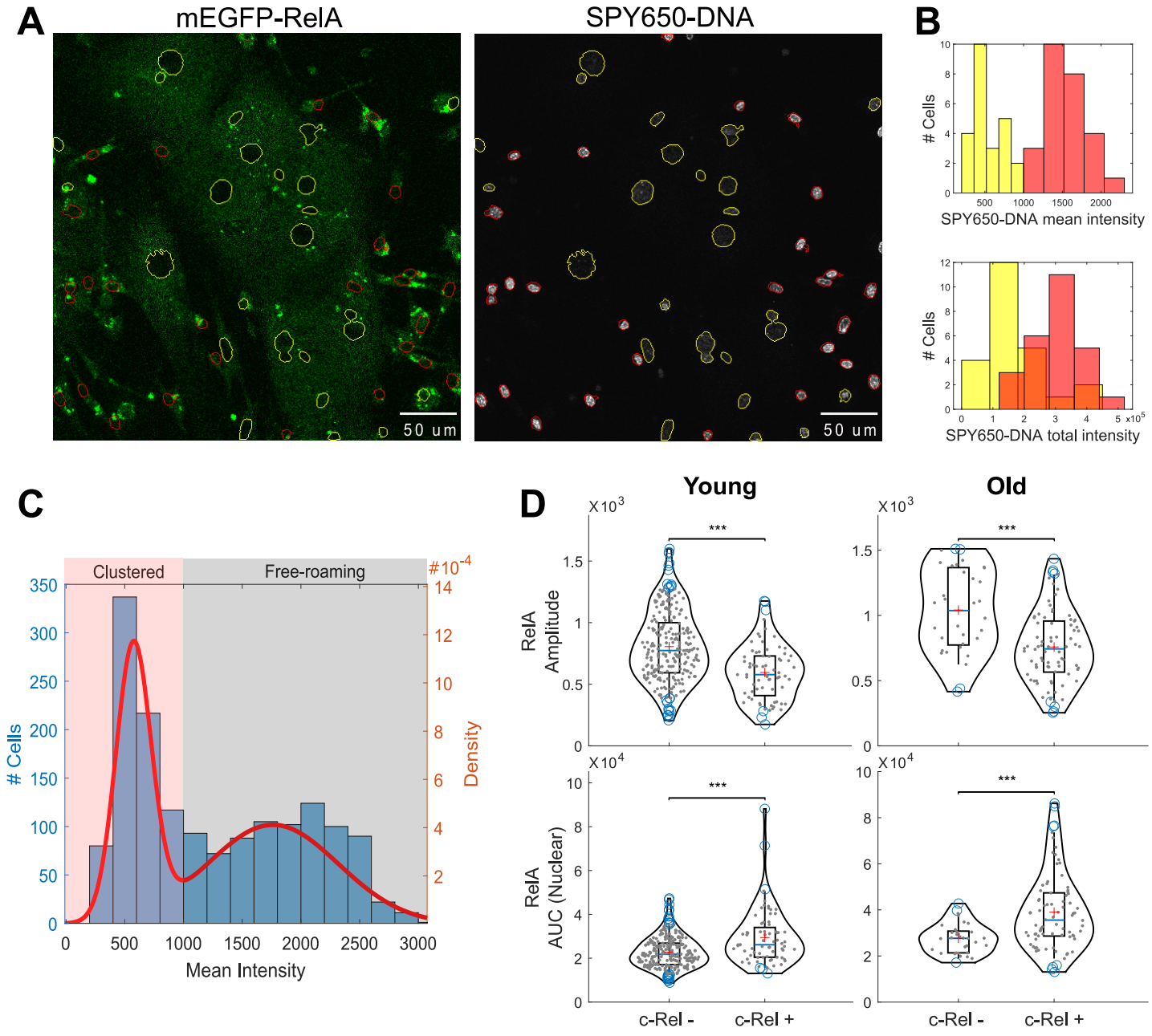


**Supplemental Figure S12. Microglia subsets with characteristic morphology, DNA dye intensity, c-Rel expression, and RelA signaling (related to Figure 6).**

(A) Classification of microglia based on mean intensity of the SPY650-DNA dye. Representative images of clustered microglia (yellow nuclear boundaries) and free-roaming microglia (red nuclear boundaries) from an old green-red DKI reporter mouse. The clustered microglia have mean intensity values of the DNA dye generally lower than a threshold, whereas the free-roaming microglia have values higher than the threshold. Scale bar, 50 μm. (B) The distributions of mean (upper) and total integrated (lower) intensities of the DNA dye show that the mean intensity distinguishes the two cell subsets better than the total intensity. (C) The distribution of the DNA dye mean intensity over the full dataset is fit by two Gaussians. (D) Violin plots show the comparison of amplitude and AUC of RelA signaling in c-Rel expressing versus non-expressing microglia from the young and old green-red DKI mice. *** $p < 0.0001$ from Mann-Whitney U test.

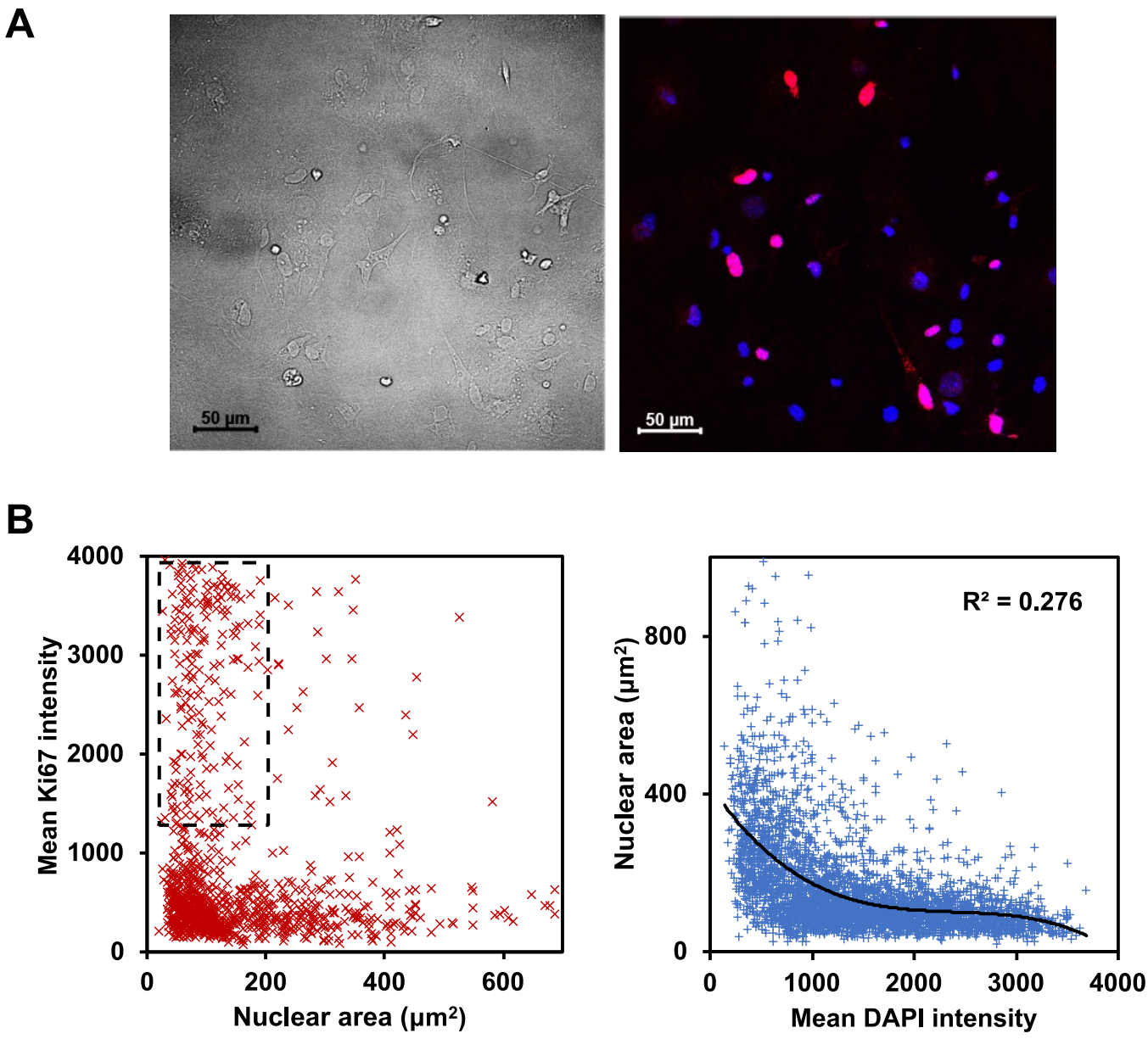


**Supplemental Figure S13. Microglia from C57BL/6 show similar features of microglia subsets in terms of morphology and DNA dye intensity as observed in green-red DKI mice (related to Figure 6).** (A) Microglia were isolated from C57BL/6 mice and subject to immunostaining on culture day 7. Brightfield (left) and fluorescence (right) images. DAPI in blue. Ki67 in red. Scale bar, 50 µm. (B) Left: Ki67 fluorescence intensity versus nuclear area of microglia. The dashed region marks the small proliferating cells. Right: Nuclear area versus mean DAPI intensity of microglia. The trend line shows a third-order polynomial fit of the data.